IEEE Access
Multidisciplinary | Rapid Review | Open Access Journal

Received November 3, 2018, accepted November 17, 2018, date of publication November 21, 2018,
date of current version December 27, 2018.

Digital Object Identifier 10.1109/ACCESS.2018.2882544

Linear Optimal Signal Designs for Multi-Color MISO-VLC Systems Adapted to CCT Requirement

YE XIAO, YI-JUN ZHU, (Member, IEEE), YAN-YU ZHANG, AND ZHENG-GUO SUN
National Digital Switching System Engineering and Technological Research Center, Zhengzhou 450000, China

Corresponding author: Yi-Jun Zhu (yijunzhu1976@outlook.com)

This work was supported by the China National Science Foundation Council under Grant 61671477.

ABSTRACT In visible light communications (VLC), multi-color light emitting diodes (LEDs) have higher modulation bandwidth and better chromatic property compared with traditional phosphor-converted LEDs. For multi-color multi-input single-output (MISO) VLC systems, multiple colors of one LED are not independent with each other since they are limited jointly with chromaticity constraint. In this paper, we develop a novel linear optimal signal constellation (LOSC) for three-color LEDs and four-color LEDs to maximize the minimum Euclidean distance of received signal constellation under lighting constraints. The main signal design problem is formulated as a max–min optimization problem with continuous variables and discrete variables. To solve this problem, we disassemble it into two parts. In the inner part, we develop a linear optimal signal structure under maximum likelihood detection criterion for the fixed average optical power of each color. In the outer part, we transform the non-convex optimization problem into several convex optimization problems with polar coordinate transformations and slack variables. Combining these two parts, our proposed LOSC design scheme shows a lower computation complexity than the exhaustive search scheme. For different given correlated color temperature (CCT) values, the LOSC would always provide an efficient signal design method adaptively. Simulation results demonstrate that our proposed LOSC achieves better bit error rate performances than the conventional schemes.

INDEX TERMS Visible light communication (VLC), multi-color LED, multiple-input-multiple-output (MIMO), constellation design, MacAdam ellipse, correlated color temperature (CCT), convex optimization.

I. INTRODUCTION

Illumination devices are now in tremendous demand and serve as a crucial part in the modern society. Visible light communications (VLC) emerge as the times require and serve as strong complement of radio frequency (RF) wireless communications [1]–[3]. At the moment, manufacture techniques of light emitting diodes (LEDs) have made progressive strides. As the new generation of illumination devices, LEDs are energy-efficient, environmentally friendly and low-cost, thus they are extensively utilized in dwelling places, office blocks and laboratories, etc [4]–[6]. Benefited from the far and wide employment of LEDs, VLC has become a promising short-range wireless communication technology [7]–[9].

In VLC systems, LED devices combine signal transmission and fundamental illumination together. Conventional white LEDs are mostly phosphor-converted LEDs (pc-LEDs) whose bandwidth is very narrow, ranging from several MHz to 30MHz for different pc-LEDs. Recently, the LEDs consisting of multi-color chips are increasingly used, especially red-green-blue LEDs (RGB-LEDs) and red-amber-green-blue LEDs (RAGB-LEDs). They accomplish white light illumination by mixing multiple monochromatic lights together and their modulation bandwidth can achieve several times larger than pc-LEDs [10]. Although multi-color LEDs are more expensive and sophisticated, their higher modulation bandwidth and natural multi-channel properties show quite large potential of high-rate data transmission. Besides, with the property of adjustable chromaticity, multi-color LEDs could always provide the most appropriate color temperature for indoor lighting.

Based on the advantageous properties of multi-color LEDs, multi-input multi-output (MIMO) technique can be naturally used in multi-color VLC systems [11], [12]. Unlike the

conventional decoupled signal constellation (DSC) in wavelength division multiplexing (WDM) which modulate monochromatic signal of each LED chip independently, the interference between multiple colors and joint chromaticity requirements need to be considered in multi-color MIMO VLC systems [15], [16]. Previously, a series of relative works have been done about these issues. In [17], the optical power allocation scheme for pulse amplitude modulation (PAM) modulation in MIMO-VLC systems was studied under illumination constraints. Moreover, due to human eyes could not distinguish small color differences, some average optical power allocation schemes are further proposed in a dynamic chromaticity range with considering the interference between adjacent colors [18], [19]. Specifically, the MISO technique is also a practical choice and some effective constellations for MISO VLC systems have been designed [20]. However, these researches merely adopted ordinary PAM modulation which in fact had not brought the property of multi-color LEDs into full use.

As the color shift keying (CSK) modulation scheme has been studied for a long time, the IEEE 802.15.7 CSK physical layer standard specified the CSK format for RGB-LEDs [21] and the issues related to the symbol mapping of three color CSK were promoted in numerous researches [22]–[24]. It should be known that the chromaticity of the white light from RGB-LEDs has one-to-one correspondence with three color optical intensities, however, the chromaticity of the white light from multi-color LEDs (more than 3 colors) corresponds to many possible color intensity proportions. Hence traditional CSK is unsuitable to be used in multi-color (more than 3 colors) VLC systems. Although R. Singh *et al.* has tried to propose an enhanced CSK scheme which uses up to three colors at one time to achieve four-color CSK [25], it still didn't use up all four colors essentially. Besides, the objective chromaticity of mixed white light from CSK modulation stays unchangeable which makes CCT values of illuminance resources cannot be adjusted as one wishes [26], [27]. Most importantly, existing optimal CSK design method has high design complexity [28]. For these reasons, our aim in this work is to design the appropriate multi-color intensity signal constellation for MISO-VLC systems adapted to CCT requirements under multiple lighting constraints.

Our proposed scheme in this work aims at providing a practical signal design method for multi-color MISO-VLC systems under multiple lighting constraints. As multi-color LEDs can work as reliable light illuminating devices and afford high speed data transmission, our method is applicable in indoor intelligent family network for the low-cost access and high-speed devices interaction. In outdoor scenarios, there are also various applications such as intelligent traffic lighting systems and underwater wireless communications etc [10]. For example, in the underwater scenario, optical turbulence causes fluctuations and fading on the received optical signal. Thus, multi-color LEDs would be effective to mitigate turbulence effects due to its high diversity property.

In this paper, the main contributions of this paper are summarized as follows:

- The signal design problem for multi-color VLC system is formulated to maximize the minimum Euclidean distance MED) of received signal constellation with multiple lighting constraints, which is a max-min optimization problem mixed with continuous variables and discrete variables.
- For any fixed average optical power, the objective function of this problem is rewritten into a linear function to get the linear optimal signal structure.
- Based on our designed signal structure, the non-convex optimization problem is turned into several convex optimization problems with polar coordinate transformations and slack variables.
- Compared with the high computation complexity of the exhaustive search algorithm, the proposed linear optimal signal design owns less complexity, which means strong practicability in real-time processing.

The remainder of this paper is laid out as follows: Section II mainly introduces the system model and our optimization problem. Section III indicates the linear optimal signal structure and a convex optimization method is used to gain the optimal average optical power under multiple lighting constraints. Performance comparison and simulation results are demonstrated in Section IV and conclusions are drawn out in Section V.

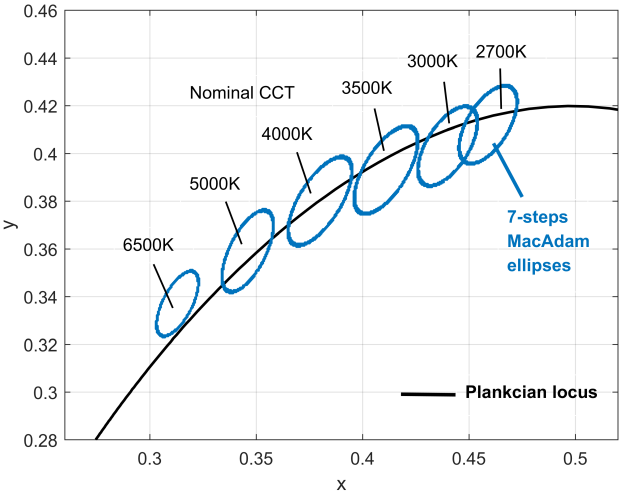

FIGURE 1. Graphical representation of the chromaticity specification of solid state lighting products on the CIE 1931 chromaticity diagram.

II. SYSTEM MODEL

A. COLOR CHARACTERISTICS OF MULTI-COLOR LED

To quantify the physical pure colors and demonstrate physiological perceived colors in human vision, the International Commission on Illumination (CIE) created the first defined quantitative color space which was called CIE 1931 XYZ space (shown in Fig.1) in 1931 [30]. The black curve in the diagram is Planckian locus which demonstrates the color of an incandescent black body would take as the black

body temperature changes. The correlated color temperature (CCT) is defined as the temperature of one Planckian radiator whose perceived color most closely resembles a given stimulus at the same condition [31].

Since white light chromaticity coordinate can be synthesized from several monochromatic light coordinates, based on Grassmann's laws of additive color mixture [32], the chromaticity coordinate of mixed white light $(\hat{x}, \hat{y})$ is calculated by multiple color coordinates (x_i, y_i) as

$$(\hat{x}, \hat{y}) = \left(\frac{\mathbf{a}^T\mathbf{\Phi}}{\mathbf{b}^T\mathbf{\Phi}}, \frac{\mathbf{1}^T\mathbf{\Phi}}{\mathbf{b}^T\mathbf{\Phi}}\right) = \left(\frac{\sum_{i=1}^{N}\frac{x_i}{y_i}\Phi_i}{\sum_{i=1}^{N}\frac{1}{y_i}\Phi_i}, \frac{\sum_{i=1}^{N}\Phi_i}{\sum_{i=1}^{N}\frac{1}{y_i}\Phi_i}\right), \quad (1)$$

where $\mathbf{a} = \left[\frac{x_1}{y_1}, \frac{x_2}{y_2}, \cdots, \frac{x_N}{y_N}\right]^T$, $\mathbf{b} = \left[\frac{1}{y_1}, \frac{1}{y_2}, \cdots, \frac{1}{y_N}\right]^T$ are coefficient vectors, $\mathbf{\Phi} = [\Phi_1, \Phi_2, \cdots, \Phi_N]^T$ is the average optical power vector for N colors.

Researches show that human eyes are unable to distinguish the small color difference in a limited chromaticity area called MacAdam ellipses. ξ-step ($\xi \geqslant 1$) MacAdam ellipses are the different sizes of ellipses in practical use which can be written as

$$g_{11}dx^2 + 2g_{12}dxdy + g_{22}dy^2 = \xi^2, \quad (2)$$

where g_{11}, g_{12} and g_{22} are constant coefficients to describe the orientation and size of ellipses, dx and dy are the differences of x and y coordinates between the points on the ellipse border and the center point of ellipse.

On account of these studies, the American National Standard Institute (ANSI) developed an Electric Lamps standard in 2008 [33]. It suggested that the chromaticity tolerance of solid state lighting products (like LEDs) should be limited in 7-steps MacAdam ellipses. The chromaticity specification of nominal CCT values in this standard is also shown in Fig. 1.

B. MULTI-COLOR MISO-VLC SYSTEM

In multi-color VLC systems, we consider N-bit multi-color signal symbols are totally transmitted, the transmitted symbol vector of N colors is $\boldsymbol{\gamma} = [\gamma_1, \gamma_2, \cdots, \gamma_N]^T \in \mathbf{\Gamma}_{2^N}$ and the symbol collection at the transmitter side is $\mathbf{\Gamma}_{2^N} = \left\{\boldsymbol{\gamma}_0, \cdots, \boldsymbol{\gamma}_{2^N-1}\right\} \in \mathbb{Z}_+^T$..

At the transmitter side, we allocate optical intensity q_i and direct-current (DC) component ϕ_{d_i} to the ith bit of signal. $\mathbf{q} = [q_1, q_2, \cdots, q_N]^T$ is the allocated optical power vector for N bits. The direct-current (DC) component vector $\boldsymbol{\phi_d} = [\phi_{d_1}, \phi_{d_2}, \cdots, \phi_{d_N}]^T$ is added to N bits signal to guarantee the constellation to be non-negative and not superposed. Hence the ith element of transmitted optical intensity signal vector $\mathbf{s} = [s_1, s_2, \cdots, s_N]^T \in \mathcal{S}$ is $s_i = q_i\gamma_i + \phi_{d_i}$, $\gamma_i \in \{0, 1\}$. $\mathcal{S} = \{\mathbf{s}_1, \mathbf{s}_2, \cdots, \mathbf{s}_L\}$ is the signal constellation at the transmitter side. $L = |\mathcal{S}| = 2^N$ is the cardinality of $\mathcal{S}$ which denotes the constellation size. In addition, the average optical power vector $\mathbf{\Phi}$ which determines the illumination chromaticity can be calculated by $\mathbf{\Phi} = \frac{1}{L}\sum_{j=1}^{L}\mathbf{s}_j = \frac{1}{2}\mathbf{q} + \phi_d$.

At the receiver side, mixed white light intensity signal is detected by a photo-detector (PD), the received signal can be written as

$$r = \mathbf{h}^T\mathbf{s} + z, \quad (3)$$

where r represents the received intensity signal scalar. $\mathbf{h} = [h_1, h_2, \cdots, h_N]^T$, h_i represents the VLC channel gain from the ith chip to the PD receiver. The channel matrix $\mathbf{h}$ is known at the transmitter side with the help of feedback channel [34]. z is the real valued additive white Gaussian noise (AWGN), $z \sim N\left(0, \sigma^2\right)$ [5]. Notably, since the diffuse light component is much lower than the weakest line-of-sight (LOS) component received, only LOS components are considered [35]. At last, the received constellation without noise can be written as $\mathcal{R} = \{r_1, r_2, \cdots, r_L\}$, $r = \sum_{i=1}^{N} h_i\left(q_i\gamma_i + \phi_{d_i}\right)$. We denote $p_i = h_iq_i$, $\psi_{d_i} = h_i\phi_{d_i}$ and $\Psi_i = h_i\Phi_i$, corresponding vectors are $\mathbf{p} = [p_1, p_2, \cdots, p_N]^T$, $\boldsymbol{\psi_d} = [\psi_{d_1}, \psi_{d_2}, \cdots, \psi_{d_N}]^T$ and $\mathbf{\Psi} = [\Psi_1, \Psi_2, \cdots, \Psi_N]^T$. So there is $r = \mathbf{p}^T \cdot \boldsymbol{\gamma} + \mathbf{1}^T\boldsymbol{\psi_d}$ and $\mathbf{\Psi} = \frac{1}{2}\mathbf{p} + \boldsymbol{\psi_d}$. Our goal in this paper is to design the optimal $\mathbf{\Phi}$, $\mathbf{q}$ and $\boldsymbol{\phi_d}$ to attain the maximized MED of the received signal constellation under multiple lighting constraints.

III. PROBLEM FORMULATION AND OPTIMIZATION SCHEME

A. FORMULATION OF OPTIMIZATION PROBLEM

Multi-color LEDs are the most crucial devices in multi-color MISO-VLC systems. To achieve wireless communication and indoor illumination at the same time, as transmitters, multi-color LEDs should satisfy several illumination and chromaticity constraints.

In this paper, there are following constraints considered:

1) TOTAL OPTICAL POWER CONSTRAINT

At the transmitter side, multiple chips illuminate several different monochromatic lights and these lights are mixed together to compose a white light. To guarantee high-quality indoor illumination, the mixed white light is obliged to be unflickering. So the total optical power constraint should be satisfied:

$$\mathbf{1}^T\mathbf{\Phi} = \sum_{i=1}^{N}\Phi_i = P_t, \quad (4)$$

where $\mathbf{\Phi} = [\Phi_1, \Phi_2, \cdots, \Phi_N]^T$ is the optical power vector of N colors and P_t indicates the total average optical power (i.e. total illumination intensity).

2) CHROMATICITY CONSTRAINT

Under most circumstances, unaided eyes could not distinguish small changes of color chromaticity. As we have mentioned in Section II, the color difference could be ignored when the chromaticity coordinates of white lights locate in the same MacAdam ellipse. Thus the chromaticity constraint of CCT tolerances can be written as

$$g_{11}\left(\hat{x} - x_0\right)^2 + 2g_{12}\left(\hat{x} - x_0\right)\left(\hat{y} - y_0\right) + g_{22}\left(\hat{y} - y_0\right)^2 \leqslant \xi^2, \quad (5)$$

where (x_0, y_0) indicates the chromaticity coordinate of the center point in the MacAdam ellipse.

3) ELECTRICAL AMPLITUDE CONSTRAINT

To avoid non-linear distortion, each chip of multi-color LED ought to be at its linear dynamic range. The electrical-optical conversion coefficient is a constant and the coefficient vector is denoted as $\boldsymbol{\eta} = [\eta_1, \eta_2, \cdots, \eta_N]^T$. The electrical signal exceeding the maximum permissible amplitude $\mathbf{A_U} = \left[A_U^1, A_U^2, \cdots, A_U^N\right]^T$ would suffer clipping distortion. So the electrical amplitude constraint can be written as

$$\mathbf{0} \leqslant 2\boldsymbol{\eta} \circ \boldsymbol{\Phi} \leqslant \mathbf{A_U}, \tag{6}$$

where the notation $\circ$ denotes the Hadamard product (i.e., $(A \circ B)_{ij} = A_{ij} \times B_{ij}$), $\mathbf{0}$ is a $N \times 1$ vector.

Given knowledge of the channel matrix H, worst-case pairwise error probability (PEP) criterion is employed in this paper to optimize the signal constellation at the receiver side [36]. For a ML receiver, PEP is determined by the maximal MED of signal constellation [37]. Considering above-mentioned constraints, the main optimization problem of our research is formulated as:

$$\begin{aligned} d_{opt} = \max_{\boldsymbol{\phi_d}, \mathbf{q}} \min_{\boldsymbol{\gamma}} & d \\ \text{s.t. } & g_{11}\left(\hat{x} - x_0\right)^2 + 2g_{12}\left(\hat{x} - x_0\right)\left(\hat{y} - y_0\right) \\ & + g_{22}\left(\hat{y} - y_0\right)^2 \leqslant \xi^2, \\ & \mathbf{0} \leqslant 2\boldsymbol{\eta} \circ \boldsymbol{\Phi} \leqslant \mathbf{A_U}, \\ & \mathbf{1}^T \boldsymbol{\Phi} = P_t, \end{aligned} \tag{7}$$

where $d = |\tilde{r} - r| = \left|\mathbf{p}^T \cdot \tilde{\boldsymbol{\gamma}} - \mathbf{p}^T \cdot \boldsymbol{\gamma}\right|, \forall \boldsymbol{\gamma}, \tilde{\boldsymbol{\gamma}} \in \boldsymbol{\Gamma}, \tilde{\boldsymbol{\gamma}} \neq \boldsymbol{\gamma}$. In problem (7), $\mathbf{p} = \mathbf{h} \circ \mathbf{q}$ and $\boldsymbol{\Phi} = \frac{1}{2}\mathbf{q} + \boldsymbol{\phi_d}$. This problem is a mix of continuous variables $\boldsymbol{\phi_d}$, $\mathbf{q}$ and discrete variables $\boldsymbol{\gamma}$, so it is hard to gain a general closed-form solution. We set $\mathcal{L}(\boldsymbol{\Phi}) = \max_{\mathbf{q}} \min_{\boldsymbol{\gamma}} d$ which indicates the maximized MED of received signal constellation and first propose the linear optimal structure for any fixed $\boldsymbol{\Phi}$. Thereupon the objective function in problem (7) can be transferred into $\max_{\boldsymbol{\Phi}} \mathcal{L}(\boldsymbol{\Phi})$. With the resulting optimal $\boldsymbol{\Phi}$, we can obtain the linear optimal design algorithm.

Accordingly, we would disassemble our main optimization problem into two parts. Firstly, in the inner part, we propose a linear optimal signal structure to attain $\max_{\mathbf{q}} \min_{\boldsymbol{\gamma}} d$ with fixed $\boldsymbol{\Phi}$. Then in the outer part, we consider the optimal solution of $\boldsymbol{\Phi}$ to attain $\max_{\boldsymbol{\Phi}} \mathcal{L}(\boldsymbol{\Phi})$ under multiple lighting constraints. Our proposed LOSC design scheme would be obtained after combining these two parts.

B. LINEAR SIGNAL STRUCTURE WITH FIXED AVERAGE POWER

Before proposing the LOSC designs for multi-color LEDs with high quality indoor illumination and communication requirements, a linear signal structure is brought forward for any fixed average optical power of multiple colors. This optimization problem is summarized as

$$\begin{aligned} \mathcal{L}(\boldsymbol{\Phi}) = \max_{\mathbf{q}} \min_{\boldsymbol{\gamma}} & d \\ \text{s.t. } & \boldsymbol{\psi_d} + \frac{1}{2}\mathbf{p} = \boldsymbol{\Psi_s}, \\ & 0 < \Psi_{s_1} \leqslant \Psi_{s_2} \leqslant \cdots \leqslant \Psi_{s_N}, \end{aligned} \tag{8}$$

where $d = \left|\mathbf{p}^T \cdot \tilde{\boldsymbol{\gamma}} - \mathbf{p}^T \cdot \boldsymbol{\gamma}\right|, \forall \boldsymbol{\gamma}, \tilde{\boldsymbol{\gamma}} \in \boldsymbol{\Gamma}, \tilde{\boldsymbol{\gamma}} \neq \boldsymbol{\gamma}$. $\boldsymbol{\Psi_s}$ equals to $\boldsymbol{\Psi}$ permuted in ascending order. Meanwhile, the order of p_i in $\mathbf{p}$ and ψ_{d_i} in $\boldsymbol{\psi_d}$ also correspond to $\boldsymbol{\Psi_s}$. Since $\boldsymbol{\Psi} = \mathbf{h} \circ \boldsymbol{\Phi}$, $\boldsymbol{\Phi_s}$ represents the correspondingly average optical power related to sorted $\boldsymbol{\Psi_s}$. As we set $\mathbf{e} = \tilde{\boldsymbol{\gamma}} - \boldsymbol{\gamma}$, $\mathbf{e} = [e_1, e_2, \cdots, e_N]^T$ is the possible error vector, this objective function can be simplified as $\max_{\mathbf{q}} \min_{\mathbf{e}} \left|\mathbf{p}^T \cdot \mathbf{e}\right|$. Since the objective function in problem (8) is a mix of continuous variables p_i and discrete variables e_i, it is hard to derive a closed-form solution of problem (8). Here we consider the power allocation for N-bit symbols so that the symbol error $e_i \in \{0, \pm 1\}$. Our goal in this section is to find the optimal allocated optical power $\mathbf{q}$ and DC bias ϕ_d to maximize MED $\min_{\mathbf{e}} d$ which is denoted as d_{opt}. Noted that $\min_{\mathbf{e}} d$ is independent of ϕ_d.

Here we would mainly study the optimal schemes for two particular cases $N = 3$ and $N = 4$. Considering the RGB-LEDs and RGBY-LEDs are most extensively used multi-chip LEDs, it is meaningful for the occasions of $N = 3$ and $N = 4$ to be studied and practically utilized.

We first propose the linear optimal signal structure for RGB-LEDs (i.e., $N = 3$) as follows.

Theorem 1: In a three-color MISO-VLC system, the optimal allocated optical power $\mathbf{q}^*$ and DC bias $\boldsymbol{\phi}_{\boldsymbol{d}}^*$ of problem (8) is as follows: When $\frac{\Psi_{s_i}}{2^{i-1}} = \min\left\{\Psi_{s_1}, \frac{\Psi_{s_2}}{2}, \frac{\Psi_{s_3}}{4}\right\}$, $i = 1, 2, 3$, there are $\mathbf{q}^* = \mathbf{m} \cdot \frac{\Psi_{s_i}}{2^{i-2}h_i}$, $\boldsymbol{\phi}_{\boldsymbol{d}}^* = \boldsymbol{\Phi_s} - \mathbf{m} \cdot \frac{\Psi_{s_i}}{2^{i-1}h_i}$, $\mathbf{m} = [1, 2, 4]^T$ and $d_{opt} = \frac{\Psi_{s_i}}{2^{i-2}}$. The received constellations of this linear optimal structure are equidistant. ■

The proof of Theorem 1 is given in Appendix A.

According to Theorem 1, we would draw out some conclusions:

1) The linear optimal signal structure for $N = 3$ is only determined by the received optical power vector $\boldsymbol{\Psi_s}$. As the minimum element of $\left\{\Psi_{s_1}, \frac{\Psi_{s_2}}{2}, \frac{\Psi_{s_3}}{4}\right\}$ varies, the values of optimal allocated optical power $\mathbf{p}$ are different, thereby the DC bias $\boldsymbol{\phi_d}$ and d_{opt} also change.
2) Distances of optimal received constellation for $N = 3$ are always equivalent. No matter which element in $\left\{\Psi_{s_1}, \frac{\Psi_{s_2}}{2}, \frac{\Psi_{s_3}}{4}\right\}$ is the minimum, the ratio of allocated optical power $\mathbf{p}$ would always meet 1:2:4.

According to the optimal design for $N = 3$ in Theorem 1, the linear optimal signal structure for four-color LEDs (i.e., $N = 4$) is finally derived in Theorem 2 as follows.

Theorem 2: In a four-color MISO-VLC system, the optimal allocated optical power $\mathbf{q}^*$ and DC bias $\boldsymbol{\phi}_{\boldsymbol{d}}^*$ of problem (8) is as follows: When $\frac{\Psi_{s_i}}{2^{i-1}} = \min\left\{\Psi_{s_1}, \frac{\Psi_{s_2}}{2}, \frac{\Psi_{s_3}}{4}, \frac{\Psi_{s_4}}{8}\right\}$, $i = 1, 2, 3$, there are $\mathbf{q}^* = \mathbf{w} \cdot \frac{\Psi_{s_i}}{2^{i-2}h_i}$, $\boldsymbol{\phi}_{\boldsymbol{d}}^* = \boldsymbol{\Phi_s} - \mathbf{w} \cdot \frac{\Psi_{s_i}}{2^{i-1}h_i}$,

$\mathbf{w} = [1, 2, 4, 8]^T$ and $d_{opt} = \frac{\Psi_{s_i}}{2^{i-2}}$. The received constellations in this case are equidistant. In the situation of $i = 4$, there are two other cases. When $\frac{\Psi_{s_i}}{c_i} = \min\left\{\Psi_{s_1}, \frac{3\Psi_{s_2}}{5}, \frac{\Psi_{s_3}}{2}, \frac{3\Psi_{s_4}}{7}\right\}$, $\mathbf{c} = \left[1, \frac{5}{3}, 2, \frac{7}{3}\right]^T$,

- if $\Psi_{s_4} > \frac{8\Psi_{s_i}}{3c_i}$, the distances of optimal constellations are equivalent. There are $\mathbf{q}^* = \mathbf{w} \cdot \frac{\Psi_{s_4}}{4h_4}$, $\boldsymbol{\phi}_d^* = \boldsymbol{\Phi}_\mathbf{s} - \mathbf{w} \cdot \frac{\Psi_{s_4}}{8h_4}$, $\mathbf{w} = [1, 2, 4, 8]^T$ and $d_{opt} = \frac{\Psi_{s_4}}{4}$.
- if $\Psi_{s_4} \leqslant \frac{8\Psi_{s_i}}{3c_i}$, the distances of optimal constellations are in-equivalent. There are $\mathbf{q}^* = \mathbf{c} \cdot \frac{2\Psi_{s_i}}{c_i h_i}$, $\boldsymbol{\phi}_d^* = \boldsymbol{\Phi}_\mathbf{s} - \mathbf{c} \cdot \frac{\Psi_{s_i}}{c_i h_i}$, $\mathbf{c} = \left[1, \frac{5}{3}, 2, \frac{7}{3}\right]^T$ and $d_{opt} = \frac{2}{3c_i}\Psi_{s_i}$. ■

The proof of Theorem 2 is given in Appendix B.

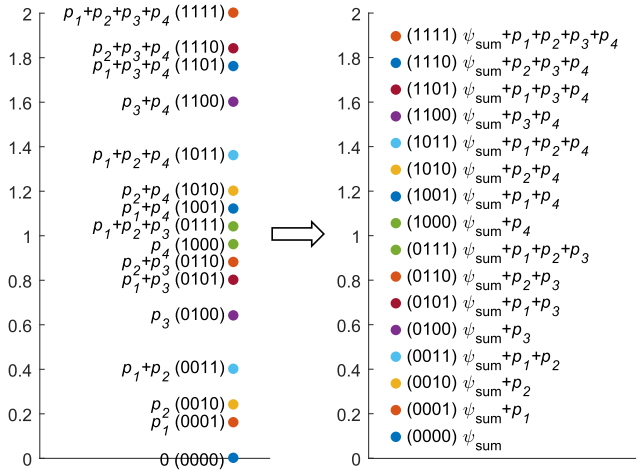

FIGURE 2. The signal constellation comparison when $\frac{\bar{\Psi}_{s_2}}{2} = \min\left\{\frac{\bar{\Psi}_{s_i}}{2^{i-1}}\right\}$. $\bar{\boldsymbol{\Psi}}_\mathbf{s} = [0.08, 0.12, 0.32, 0.48]^T$.

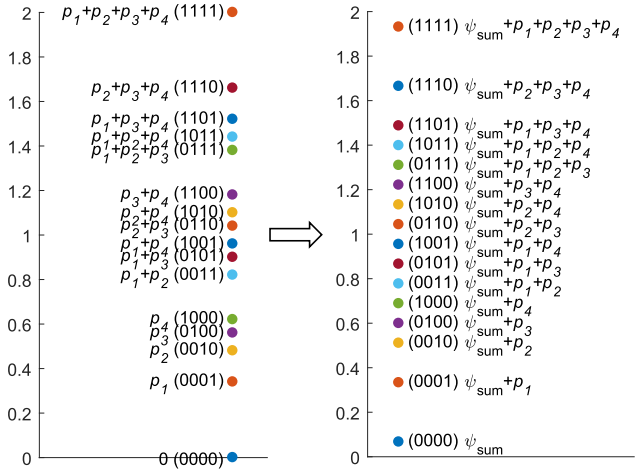

FIGURE 3. The signal constellation comparison when $\frac{\bar{\Psi}_{s_4}}{8} = \min\left\{\frac{\bar{\Psi}_{s_i}}{2^{i-1}}\right\}$ and $\frac{\bar{\Psi}_{s_1}}{c_1} = \min\left(\frac{\bar{\Psi}_{s_l}}{c_l}\right)$, $\frac{\bar{\Psi}_{s_1}}{c_1} > \frac{\bar{\Psi}_{s_4}}{8}$. $\bar{\boldsymbol{\Psi}}_\mathbf{s} = [0.17, 0.24, 0.28, 0.31]^T$.

Next, we would exemplify two typical possible occasions of $\boldsymbol{\Psi}_\mathbf{s}$ for comparing conventional signal constellation and our linear optimal constellation in Fig. 2 and Fig. 3. For simplicity, here we denote $\psi_{\text{sum}} = \psi_{d_1} + \psi_{d_2} + \psi_{d_3} + \psi_{d_4}$. Noted that the binary symbols in brackets and mathematical formulas beside constellation points in diagrams are transmitted codewords and corresponding intensity values, respectively.

When the normalized $\bar{\boldsymbol{\Psi}}_\mathbf{s} = [0.08, 0.12, 0.32, 0.48]^T$ (i.e., $\frac{\bar{\Psi}_{s_2}}{2} = \min\left\{\bar{\Psi}_{s_1}, \frac{\bar{\Psi}_{s_2}}{2}, \frac{\bar{\Psi}_{s_3}}{4}, \frac{\bar{\Psi}_{s_4}}{8}\right\}$), Fig. 2 depicts constellation diagrams of conventional DSC on the left and our designed LOSC on the right. Since the DSC is only designed for satisfying chromaticity constraints without utilizing the multidimensional joint property of multiple colors, the MED of our designed LOSC is obviously larger than DSC so that our scheme would show better performance.

Meanwhile, constellation diagrams of DSC and LOSC at the time of $\bar{\boldsymbol{\Psi}}_\mathbf{s} = [0.17, 0.24, 0.28, 0.31]^T$ (i.e., $\frac{\bar{\Psi}_{s_4}}{8} = \min\left\{\bar{\Psi}_{s_1}, \frac{\bar{\Psi}_{s_2}}{2}, \frac{\bar{\Psi}_{s_3}}{4}, \frac{\bar{\Psi}_{s_4}}{8}\right\}$) are also demonstrated in Fig. 3. In this occasion, the optimal constellation of our scheme is non-equidistant unlike above-mentioned equidistant constellations. Apparently, our proposed LOSC also owns larger MED than conventional DSC.

According to Theorem 2, there are some conclusions summarized as follows:

1) The linear optimal signal structure for $N = 4$ when $i = 1, 2, 3$ resembles the scheme for $N = 3$. The ratio of allocated optical power $\mathbf{p}$ would always meets 1:2:4:8. However, this equidistant scheme not always achieves the optimal constellation.
2) When $\frac{1}{8}\Psi_{s_4}$ is the minimum in $\left\{\Psi_{s_1}, \frac{\Psi_{s_2}}{2}, \frac{\Psi_{s_3}}{4}, \frac{\Psi_{s_4}}{8}\right\}$, there exists some optimal non-equidistant occasions. The ratio of allocated optical power $\mathbf{p}$ in these cases would always meet 3:5:6:7 and $d_{opt} = \frac{1}{3}p_1 = \frac{2}{3c_i}\Psi_{s_i}$. What is worth mentioning is that these non-equidistant occasions only appear when $N = 4$ and the equidistant scheme still works and has a good performance even though it couldn't achieve the maximal MED.

Noted that although our linear optimal scheme is mainly proposed for three-color LEDs and four-color LEDs, the problem (8) is also able to be utilized for an arbitrary N. Since there are $N!$ cases to be compared for a specific $\boldsymbol{\Psi}$ in problem (8), theoretical methods would not show much advantage in deriving the optimal solution for $N > 4$. In that cases, numerical search approaches are more suitable to be used for a large N which is not discussed in this paper.

C. OPTIMIZATION OF ALLOCATED AVERAGE POWER

Above subsection states an linear optimal signal structure when the average optical power of each chip is fixed. In this part, the optimization of $\boldsymbol{\Phi}$ is considered under multiple lighting constraints. Therefore, this optimization problem is equivalent to finding the optimal $\boldsymbol{\Phi}$ which maximizes $\mathcal{L}(\boldsymbol{\Phi})$. In multi-color MISO-VLC systems, the impact of channel vector $\mathbf{h}$ equals to scaling the amplitude of each transmitted signal and the scaling of $\mathbf{h}$ could be imposed primarily to the value of average optical power $\boldsymbol{\Phi}$. After the optimization is completed based on $\boldsymbol{\Psi}_\mathbf{s}$, the impact of $\mathbf{h}$ can be removed to derive the optimal solutions. So we would omit

the calculation process of $\mathbf{h}$ in the following sections without losing generality.

As the exhaustive search requires too much calculation resources, to promise affordable complexity, we would propose a method to attain the global optimal solutions by transferring the non-convex problem into several convex problems. Since the first elliptical constraint in problem (7) is non-convex, the polar coordinate of ellipse is adopted to transform the expression in Eq. (2). as [38]. So the elliptical constraint can be simplified as

$$\begin{cases} m^2+n^2 \leqslant \left(\xi \mathbf{b}^T \mathbf{\Phi}\right)^2, \\ 0 \leqslant t \leqslant \xi \mathbf{b}^{\mathbf{T}} \mathbf{\Phi}, \\ m=\dfrac{1}{\alpha}\left[\left(\mathbf{a}^T-x_0\mathbf{b}^T\right)\cos\theta+\left(\mathbf{1}^T-y_0\mathbf{b}^T\right)\sin\theta\right]\mathbf{\Phi}, \\ n=\dfrac{1}{\beta}\left[\left(\mathbf{1}^T-y_0\mathbf{b}^T\right)\cos\theta+\left(\mathbf{a}^T-x_0\mathbf{b}^T\right)\sin\theta\right]\mathbf{\Phi}. \end{cases} \tag{9}$$

where

$$\begin{cases} \alpha=\sqrt{\dfrac{2}{(g_{11}+g_{22})-\sqrt{(g_{11}-g_{22})^2+4g_{12}^2}}}, \\ \beta=\sqrt{\dfrac{2}{(g_{11}+g_{22})+\sqrt{(g_{11}-g_{22})^2+4g_{12}^2}}}. \end{cases} \tag{10}$$

The rotated angle θ is calculated by

$$\theta=\begin{cases} 0, & \text{for } g_{12}=0 \text{ and } g_{11}<g_{22}; \\ \dfrac{\pi}{2}, & \text{for } g_{12}=0 \text{ and } g_{11}>g_{22}; \\ \dfrac{1}{2}\cot^{-1}\left(\dfrac{g_{11}-g_{22}}{2g_{12}}\right), & \text{for } g_{12}\neq 0 \text{ and } g_{11}<g_{22}; \\ \dfrac{\pi}{2}+\dfrac{1}{2}\cot^{-1}\left(\dfrac{g_{11}-g_{22}}{2g_{12}}\right), & \text{for } g_{12}\neq 0 \text{ and } g_{11}>g_{22}. \end{cases} \tag{11}$$

It could be observed that $\mathcal{L}(\mathbf{\Phi})$ varies from the permutation of $\Psi_1, \Psi_2, \cdots, \Psi_N$. We find that the objective function in this optimization problem is not convex, nevertheless, it is linear in each independent $\mathbf{\Phi}$-region. On account of this feature, the optimization problem can be transferred into some convex optimization problems with different linear objective functions. The first constraint in problem (9) is defined in a Lorentz cone so that this problem is transferred to a second-order conic program (SOCP) with respect to $\mathbf{\Phi}$ and t. Finally, the optimization problem can be disassembled into several different convex problems as

$$\begin{aligned} &\max_{\mathbf{\Phi}} \ \mathcal{L}(\mathbf{\Phi}) \\ &\text{s.t. } m^2+n^2 \leqslant t^2, \\ &\quad 0 \leqslant t \leqslant \xi \mathbf{b}^T \mathbf{\Phi}, \\ &\quad m=\frac{1}{\alpha}\left[\left(\mathbf{a}^T-x_0\mathbf{b}^T\right)\cos\theta+\left(\mathbf{1}^T-y_0\mathbf{b}^T\right)\sin\theta\right]\mathbf{\Phi}, \\ &\quad n=\frac{1}{\beta}\left[\left(\mathbf{1}^T-y_0\mathbf{b}^T\right)\cos\theta+\left(\mathbf{a}^T-x_0\mathbf{b}^T\right)\sin\theta\right]\mathbf{\Phi}, \\ &\quad \mathbf{0} \leqslant 2\boldsymbol{\eta} \circ \mathbf{\Phi} \leqslant \mathbf{A_U}, \\ &\quad \mathbf{1}^T\mathbf{\Phi}=P_t. \end{aligned} \tag{12}$$

These convex problems could be numerically solved by optimization algorithms such as infeasible path-following algorithms [39]. In the following section, we would handle this problem by using the MATLAB convex optimization toolbox CVX [40]. After comparing all the suboptimal results $\mathcal{L}(\mathbf{\Phi})$ in different $\mathbf{\Phi}$-regions, we could gain the globally optimal solution of $\mathbf{\Phi}$. Finally, our proposed LOSC design scheme is worked out according to Theorem 2.

D. ALGORITHMS AND COMPLEXITY ANALYSIS

In above subsections, we concentrate on the signal structure design and the solving method of optimal problem. Next, we will specify the algorithms of our proposed scheme and the exhaustive search scheme in detail. Meanwhile, the computation complexity of these two schemes is also analysed and compared.

For multi-color MISO-VLC systems, the exhaustive search algorithm to attain the optimal received signal constellation (represented as ESC) is given as Algorithm 1.

Algorithm 1 Exhaustive Search Algorithm

1) Given the exhaustive range of $\mathbf{\Phi}$ and the computation precision ϵ, N_e is the search-costing times. Decide each $\mathbf{\Phi}_k$ ($k \in [1, 2, \cdots, N_e]$) to find the one who satisfies multiple constraints in problem (12), calculate the corresponding $\mathcal{L}(\mathbf{\Phi}_k)$. Exhaust this step for all the $\mathbf{\Phi}_k$.
2) Compare all the $\mathcal{L}(\mathbf{\Phi}_k)$, the Φ attaining the maximum value is the optimal solution.

To avoid the high computation complexity of exhaustive search in ESC, we propose the convex optimization method which owns decreased logarithmic complexity. The detailed algorithm is provided in Algorithm 2.

Algorithm 2 Convex Optimization Algorithm

1) For $\mathbf{\Phi} \in \mathcal{H}$, given the range of $d \in [d_1, d_2]$ and the computation precision ϵ, initialize $d_{\min}=d_1$ and $d_{\max}=d_2$.
2) **While** $d_{\max}-d_{\min}>\epsilon$
Set $d_t=(d_{\min}+d_{\max})/2$.
Solve the convex optimization problem (12).
If problem (12) is solvable, then set $d_{\min}=d_t$.
Otherwise, set $d_{\max}=d_t$.
end
3) Calculate all the optimal d_t in different regions. The $\mathbf{\Phi}$ corresponding to the maximum d_t is the optimal solution.

In the worst case, the iteration complexity of the problem (12) is $\mathcal{O}\left(log_2\epsilon^{-1}\right)$ where ϵ is the required accuracy of interior-point iterations. As the complexity per iteration of a SOCP problem with the interior-point method is $\mathcal{O}\left(N^{3.5}\right)$ [41], the complexity of our proposed optimization scheme in Algorithm 2 is $\mathcal{O}\left(N^{3.5}log_2\epsilon^{-1}\right)$. The complexity required by the exhaustive search method in Algorithm 1 is $\mathcal{O}\left(N_e^N\right)$ where N_e depends on the required accuracy ϵ. In Table 1 and Table 2, we list the computational operations

TABLE 1. Complexity comparison at $N = 3$.

Operations	$\epsilon = 0.1$	$\epsilon = 0.01$	$\epsilon = 0.001$	$\epsilon = 0.0001$
LOSC	155	311	466	621
ESC	10^3	10^6	10^9	10^{12}

TABLE 2. Complexity comparison at $N = 4$.

Operations	$\epsilon = 0.1$	$\epsilon = 0.01$	$\epsilon = 0.001$	$\epsilon = 0.0001$
LOSC	425	850	466	1701
ESC	10^4	10^8	10^{12}	10^{16}

of our proposed LOSC and conventional ESC with different required accuracy. It could observed that the complexity of our proposed LOSC increases logarithmically with the decrease of required accuracy while the complexity of conventional ESC increases exponentially with the decrease of required accuracy. The higher accuracy requirement, the more evident advantage of Algorithm 2. Compared to the exhaustive search method, our proposed scheme saves a lot of computational complexity which means strong practicability in the real-time processing.

IV. SIMULATIONS RESULTS

In this section, we would conduct some simulations to examine the average error performance of our proposed LOSC design scheme for RAGB-LED (i.e. $N = 4$, $N_r = N_a = N_g = N_b = 1$). The maximum forward current for each chip is 700 mA. The electrical-optical conversion coefficients for red, amber, green, blue chips are 0.021 A/lm, 0.014 A/lm, 0.005 A/lm, and 0.015 A/lm, respectively. The x-y chromaticity coordinates of RAGB color lights are given as red (0.69406, 0.30257), amber (0.59785, 0.39951), green (0.22965, 0.70992), blue (0.12301, 0.09249). In this typical indoor multi-color MISO scenario, all the chips are located in a small packaged LED such that the distances from multiple chips to the PD can be regarded as the same. Only one PD is used to detect the mixed white light illuminated from the multi-color LED. Based on [36], the channel gain is represented as

$$h_i = \frac{(m+1)\,A_R \delta_i}{2\pi D^2} \cos(\phi)^m \cos(\psi), \tag{13}$$

where the order of Lambertian emission m is given by $m = -\frac{\ln 2}{\ln(\cos\Phi_{1/2})}$, in which the half power angle of LED $\Phi_{1/2}$ is 70°, the detector area A_R is 1 cm^2, the receiver responsibility δ is 0.4 A/W, the distance D between the LED chip and PD is 2.5 m, the angle of irradiance ϕ and the angle of incidence ψ are both 10°. ML detection algorithm is adopted at the receiver side in following simulations. Besides, Table 3 shows the detailed parameters of related MacAdam ellipses in our simulations [42]. The CVX toolbox used in this work is version 3.0 and MATLAB is version 2017a.

TABLE 3. Chromaticity specification of MacAdam ellipses.

CCT	Center point	g_{11}	$2g_{12}$	g_{22}
2700K	(0.459, 0.412)	40×10^4	-39×10^4	28×10^4
3000K	(0.440, 0.403)	39×10^4	-39×10^4	27.5×10^4
3500K	(0.411, 0.393)	38×10^4	-40×10^4	25×10^4
4000K	(0.380, 0.380)	39.5×10^4	-43×10^4	26×10^4
5000K	(0.346, 0.359)	56×10^4	-50×10^4	28×10^4
6500K	(0.313, 0.337)	86×10^4	-80×10^4	45×10^4

A. COMPARISON BETWEEN PROPOSED LOSC AND CONVENTIONAL DECOUPLED SCHEME

We first compare the BER performance of our proposed LOSC design scheme with the conventional decoupled scheme and exhaustive search results. The BER is calculated by the Monte Carlo method and the length of transmitted data is set to be 10^8 in simulations. To make a fair comparison, all these signal constellations are with equal spectrum efficiency, equal average optical power and under the same lighting constraints. The main signal structures of these three schemes are summarized as follows:

1) *Proposed LOSC scheme.* The constellation $\mathcal{S}_L$ of our proposed scheme is attained based on the linear signal structure designed in Theorem 2 and the optimal $\mathbf{\Phi}$ calculated from convex optimization algorithm.
2) *Conventional DSC scheme.* Each $\mathbf{s}_i$ from $\mathcal{S}_D$ for the conventional decoupled scheme takes value from OOK (2-PAM) signal constellations independently.
3) *Exhaustive search scheme.* We exhaustively search all the possible $\mathcal{S}_E$ under constraints to gain the optimal constellation which achieves the maximized MED at the receiver side.

Our simulations compare the BER performance among different signal design schemes versus different optical signal-to-noise ratio (SNR) for two selected CCT values when $\xi = 1$ and $\xi = 7$. The SNR is defined as P_t/σ^2 where the total optical power P_t is set to be 100lm, thus all the colors have not suffered any non-linear distortion.

In Fig. 4 to Fig. 6, the BER performances of different schemes versus SNR for different CCT values (i.e, CCT = 2700 K, 3000 K, 5000 K) are shown. In Fig. 4, compared with the conventional DSC, it can be observed that our proposed LOSC provides the BER gain about 6.3 dB when $\xi = 1$ and the BER gain about 6.1 dB when $\xi = 7$ at the target of BER $= 10^{-5}$. As shown in Fig. 5, the performance gain would be about 6.2 dB and 5.8 dB when $\xi = 1$ and $\xi = 7$, respectively. Fig. 6 demonstrates BER performances for CCT = 5000K and we can observe that our proposed LOSC shows approximately 2.8 dB when $\xi = 1$ and 4.7 dB gains when $\xi = 7$ than the conventional DSC. Furthermore, when CCT = 5000K, our proposed LOSC can always gain near BER performance with optimal ESC no matter $\xi = 1$ and $\xi = 7$.

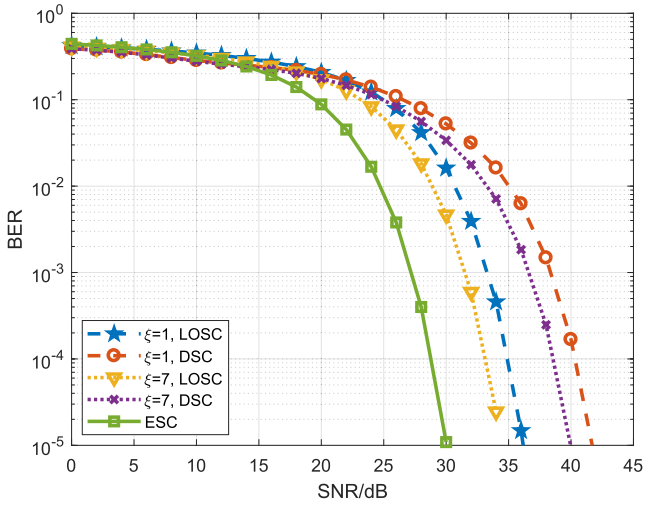

FIGURE 4. BER performance comparison of different MacAdam ellipse steps versus SNR when CCT = 2700 K.

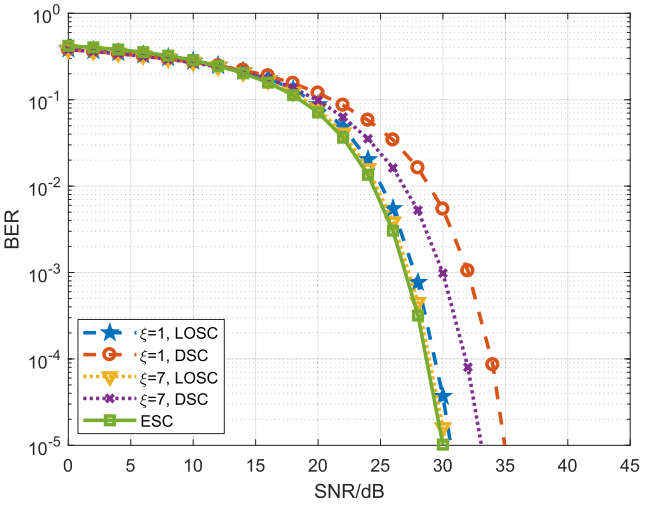

FIGURE 6. BER performance comparison of different MacAdam ellipse steps versus SNR when CCT = 5000 K.

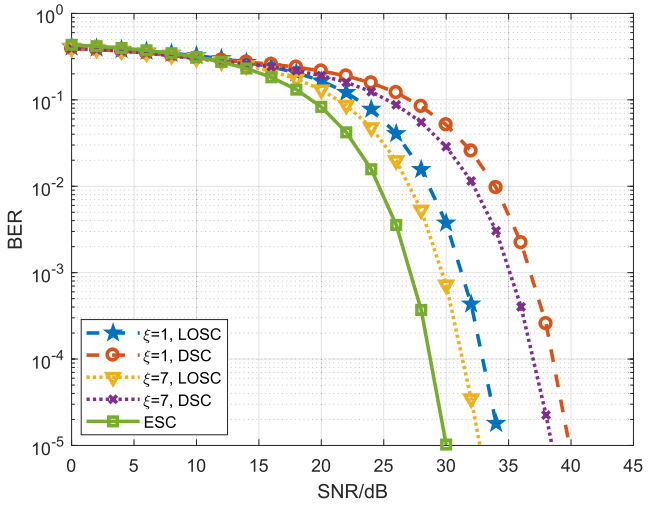

FIGURE 5. BER performance comparison of different MacAdam ellipse steps versus SNR when CCT = 3000 K.

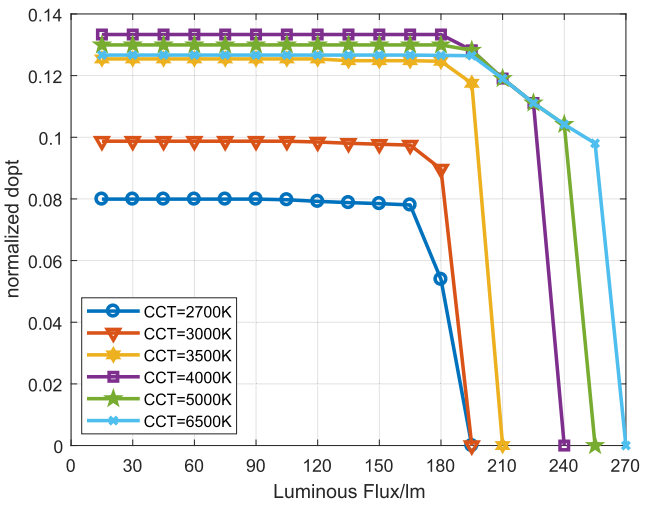

FIGURE 7. The comparison of normalized maximized MED under different luminous flux for different CCT values.

Observing from Fig. 4 to Fig. 6, both of LOSC and DSC can not compare with ESC, nevertheless, LOSC decrease much computation complexity than the exhaustive search while suffering less performance penalty than DSC. Besides, when the step of MacAdam ellipse is $\xi = 7$, we find that both of LOSC and DSC could attain better BER performances than $\xi = 1$. This is because the useable chromaticity range of 7-step ellipse is larger than 1-step ellipse, all of these schemes would gain superior signal constellations under more relaxed constraints.

B. PERFORMANCE OF PROPOSED LOSC SCHEME

To reveal the performance variation of our proposed LOSC scheme, in Fig. 7 we illustrate the normalized d_{opt} under different luminous flux. The step of MacAdam ellipse is set to be 7 and different CCT values (i.e., 2700 K, 3000 K, 3500 K, 4000 K, 5000 K, 6500 K) are considered. From Fig. 7, we can observe that all the curves stay smooth at first but then suffer a rapid decrease and finally go into zero. The reason is that higher optical power corresponds to higher forward electric current which is limited under the amplitude constraint.

Next, we mainly discuss performances of proposed LOSC before multiple colors of the LED transmitter suffer non-linear distortion. The BER performances are depicted in Fig. 8. It can be seen that the best performance of LOSC is obtained at the time of CCT = 4000 K as the BER performance approaches the optimal ESC. Furthermore, the signal design results when CCT values are 3500 K, 4000 K, 5000 K and 6500 K all demonstrate well enough performances. The performance gaps between LOSC and ESC are less than 0.9 dB when CCT values are higher than 3500 K.

We also depict the variation of four colors proportions to achieve the maximized MED versus luminous flux when CCT = 4000 K. The proportions of four colors almost remain unchanged at first which are 0.1333, 0.2667, 0.5333 and 0.0667, respectively. Then, all of the curves show

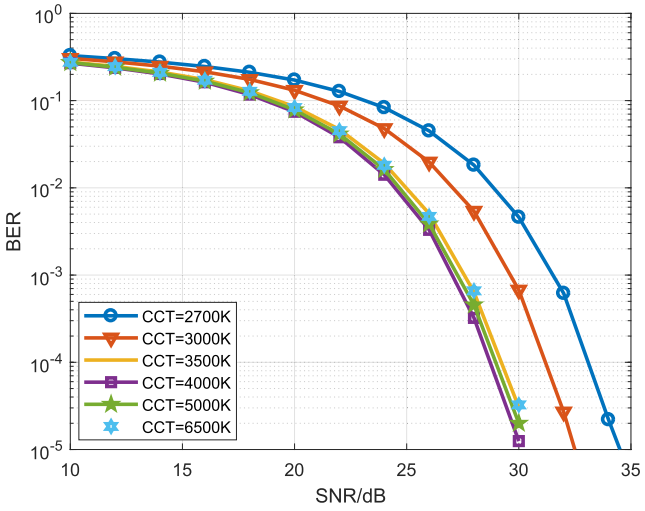

FIGURE 8. The BER performance of proposed LOSC design scheme for different CCT values.

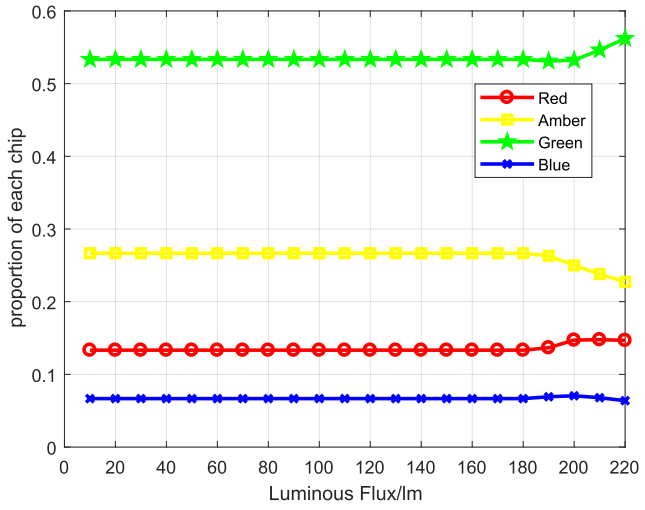

FIGURE 9. The proportion of four colors to achieve the maximized MED when CCT = 4000 K.

fluctuation to some extent because of the limitation of electrical amplitude constraint.

Simulation results show that our proposed LOSC design scheme provides efficient performance improvement than the conventional scheme and costs less computation resources despite its performance would not always be optimal. It also indicates that LOSC can always obtain more performance gain when the step of MacAdam ellipse is larger. We also come to the conclusion that LOSC with higher total optical power would suffer some degree of performance loss due to the electrical amplitude constraint of LED transmitter. In addition, the optimum communication performance of LOSC for $\xi = 7$ is attained when CCT $= 4000$ K which derives the optimal signal constellation as same as the exhaustive search.

V. CONCLUSIONS

In this paper, we have investigated a multi-color MISO-VLC system in which multi-color LEDs are utilized to transmit the VLC signal. Considering that the color mixing from multiple chips should comply certain proportions to satisfy illumination and chromaticity demands, we have developed a signal constellation to maximize MED of received signal constellation with multiple lighting constraints. Since the optimization problem consists of continuous variables and discrete variables, we disassemble it into inner part and outer part. At first, in the inner part, the linear signal constellation structure for any fixed average optical power has been attained by theoretical derivations. Then, through a series of polar coordinate transformations and the usage of slack variables, the outer non-convex problem has been reformulated as some convex problems. Optimal results of average optical power adapted to CCT values have been attained so that our proposed LOSC designs finally yield. Simulation results have testified that the performances of LOSC are better than the conventional DSC in most cases. In the future, more workable signal design schemes based on more than four colors VLC systems wait to be further investigated. Our proposed scheme in this work aims at providing a critical method of power allocation and signal design for multi-color MISO-VLC systems with different lighting constraints.

APPENDIX

A. PROOF OF THEOREM 1

In multi-color MISO-VLC systems, on the condition of $0 < \mathbf{p} \leqslant 2\boldsymbol{\Psi}_\mathbf{s}$, $0 < \Psi_{s_1} \leqslant \Psi_{s_2} \leqslant \cdots \leqslant \Psi_{s_N}$, when DC bias is left out, if we suppose that $p_i \geqslant p_j$ at the moment of $i < j$, due to $0 < p_i \leqslant 2\Psi_{s_i}$, $0 < p_j \leqslant 2\Psi_{s_j}$ and $\Psi_{s_i} \leqslant \Psi_{s_j}$, we derive that $0 < p_j \leqslant p_i \leqslant 2\Psi_{s_i}$. Thus, larger constellation distances could always be attained while swapping p_i and p_j (i.e., $p_i < p_j$). All the situation of $p_i \geqslant p_j$ would never be superior to $p_i < p_j$. Therefore, the order of $p_1, p_2, \cdots, p_N$ in the optimal received constellation is always $p_1 < p_2 < \cdots < p_N$.

For $N = 3$, the objective function in problem (8) can be rewritten as $\max_{\mathbf{p}} \min(p_1, p_2, p_3, p_2-p_1, p_3-p_1, p_3-p_2, p_2+p_3-p_1, p_1+p_3-p_2, |p_1+p_2-p_3|)$ [43]. According to the sign of $(p_1+p_2-p_3)$, there are two possible cases:

Case 1: If $p_1+p_2 > p_3$, the objective function could be simplified as $\max_{\mathbf{p}} \min(p_2-p_1, p_3-p_2, p_1+p_2-p_3)$. Firstly, if $\min_{\mathbf{e}} d = p_2-p_1$, this problem is a linear programming (LP) problem which could be written as

$$\begin{aligned} \text{LP1}: \quad & \max\, p_2 - p_1 \\ & \text{s.t. } p_2 - p_1 < p_3 - p_2, \\ & \quad p_2 - p_1 < p_1 + p_2 - p_3. \end{aligned} \tag{14}$$

On the basis of [44, Th. 2.7], since the feasible set of this problem is nonempty and bounded, it is easy to prove that the maximized d is obtained when the basic feasible solution is $\mathbf{p} = [1, \frac{3}{2}, 2]^T p_1$. Similarly, when $\min_{\mathbf{e}} d = p_3 - p_2$ or $\min_{\mathbf{e}} d = p_1 + p_2 - p_3$, we could also get the same result. Therefore, the optimal d was $d_{opt} = \frac{1}{2}p_1$.

Then this question is further simplified as maximizing p_1 subject to $\psi_{d_1}+\frac{p_1}{2}=\Psi_{s_1}, \psi_{d_2}+\frac{3}{4}p_1=\Psi_{s_2}, \psi_{d_3}+p_1=\Psi_{s_3}$ and $\psi_{d_1}, \psi_{d_2}, \psi_{d_3} \geqslant 0$. These constraints can be transferred to $0 < p_1 \leqslant \min\left(2\Psi_{s_1}, \frac{4}{3}\Psi_{s_2}, \Psi_{s_3}\right)$. As we set the constant vector $\mathbf{u}=\left[1, \frac{3}{2}, 2\right]^T$, when $\frac{\Psi_{s_i}}{u_i}=\min\left(\Psi_{s_1}, \frac{2}{3}\Psi_{s_2}, \frac{1}{2}\Psi_{s_3}\right)$, the optimal $\mathbf{p}^*=\mathbf{u}\cdot\frac{2\Psi_{s_i}}{u_i}$, $\boldsymbol{\psi}_{\boldsymbol{d}}^*=\boldsymbol{\Psi}_{\mathbf{s}}-\mathbf{u}\cdot\frac{\Psi_{s_i}}{u_i}$ and $d_{opt}=\frac{\Psi_{s_i}}{u_i}$. So the optimal $\mathbf{q}^*=\mathbf{u}\cdot\frac{2\Psi_{s_i}}{u_i h_i}$ and $\boldsymbol{\phi}_{\boldsymbol{d}}^*=\boldsymbol{\Phi}_{\mathbf{s}}-\mathbf{u}\cdot\frac{\Psi_{s_i}}{u_i h_i}$.

Case 2: If $p_1+p_2 < p_3$, the objective function could be simplified as $\max_{\mathbf{p}} \min(p_1, p_2-p_1, p_1+p_2-p_3)$. Optimizing method here resembles the case 1, the $d_{opt}=p_1$ is obtained when $\mathbf{p}=[1,2,4]^T p_1$. So d_{opt} is determined by $\min(\Psi_{s_1}, \frac{1}{2}\Psi_{s_2}, \frac{1}{4}\Psi_{s_3})$. As we set the constant vector $\mathbf{m}=[1,2,4]^T$, when $\frac{\Psi_{s_i}}{2^{i-1}}=\min\left(\Psi_{s_1}, \frac{\Psi_{s_2}}{2}, \frac{\Psi_{s_3}}{4}\right)$, the optimal $\mathbf{p}^*=\mathbf{m}\cdot\frac{\Psi_{s_i}}{2^{i-2}}$, $\boldsymbol{\psi}_{\boldsymbol{d}}^*=\boldsymbol{\Psi}_{\mathbf{s}}-\mathbf{m}\cdot\frac{\Psi_{s_i}}{2^{i-1}}$ and $d_{opt}=\frac{\Psi_{s_i}}{2^{i-2}}$. So the optimal $\mathbf{q}^*=\mathbf{m}\cdot\frac{\Psi_{s_i}}{2^{i-2}h_i}$ and $\boldsymbol{\phi}_{\boldsymbol{d}}^*=\boldsymbol{\Phi}_{\mathbf{s}}-\mathbf{m}\cdot\frac{\Psi_{s_i}}{2^{i-1}h_i}$.

Considering above two cases, no matter which element in $\left(\Psi_{s_1}, \frac{2}{3}\Psi_{s_2}, \frac{1}{2}\Psi_{s_3}\right)$ is the minimum, d_{opt} in *Case 1* always not compare with *Case 2*. So the linear optimal signal structure is as *Case 2*. The proof of Theorem 1 is completed. □

B. PROOF OF THEOREM 2

For $N=4$, based on Theorem 1, we infer that the linear optimal signal structure for $N=4$ resembles $N=3$. That is to say, when $\frac{\Psi_{s_i}}{2^{i-1}}=\min\left(\Psi_{s_1}, \frac{\Psi_{s_2}}{2}, \frac{\Psi_{s_3}}{4}, \frac{\Psi_{s_4}}{8}\right)$, $i=1,2,3,4$, there are $\mathbf{p}=\mathbf{w}\cdot\frac{\Psi_{s_i}}{2^{i-2}}$, $\boldsymbol{\psi}_{\boldsymbol{d}}=\boldsymbol{\Psi}_{\mathbf{s}}-\mathbf{w}\cdot\frac{\Psi_{s_i}}{2^{i-1}h_i}$, $\mathbf{w}=[1,2,4,8]^T$ and $d_{opt}=\frac{\Psi_{s_i}}{2^{i-2}}$. It could be proved that this scheme is feasible but it may not be the optimal scheme for $N=4$. To examine whether this deduction is correct, we assume that there exists $\hat{d}=\min d > d_{opt}$. For all the $d=|p_1e_1+p_2e_2+p_3e_3+p_4e_4|$, they will satisfy $d \geqslant \hat{d} > d_{opt}$. Noted that $\mathbf{0} < \mathbf{p} \leqslant 2\boldsymbol{\Psi}_{\mathbf{s}}$.

When $\Psi_{s_1}=\min\left(\Psi_{s_1}, \frac{\Psi_{s_2}}{2}, \frac{\Psi_{s_3}}{4}, \frac{\Psi_{s_4}}{8}\right)$, there is $p_1 > d_{opt}=2\Psi_{s_1}$ which is a contradiction. Hence $d_{opt}=2\Psi_{s_1}$.

When $\frac{\Psi_{s_2}}{2}=\min\left(\Psi_{s_1}, \frac{\Psi_{s_2}}{2}, \frac{\Psi_{s_3}}{4}, \frac{\Psi_{s_4}}{8}\right)$, there are $p_2-p_1, p_1, p_2 > d_{opt}=\Psi_{s_2}$. Because of $\Psi_{s_2} < p_1 < p_2 \leqslant 2\Psi_{s_2}$, we can get $p_2-p_1 < 2\Psi_{s_2}-\Psi_{s_2}=\Psi_{s_2}$ which is a contradiction. Hence $d_{opt}=\Psi_{s_2}$.

When $\frac{\Psi_{s_3}}{4}=\min\left(\Psi_{s_1}, \frac{\Psi_{s_2}}{2}, \frac{\Psi_{s_3}}{4}, \frac{\Psi_{s_4}}{8}\right)$, there is $d_{opt}=\frac{1}{2}\Psi_{s_3}$, $0 < p_1 < p_2 < p_3$. If $p_1+p_2 < p_3$, $0 < p_1 < p_2 < p_1+p_2 < p_3$, there is $p_3 > 4\hat{d}=2\Psi_{s_3}$ which is a contradiction. If $p_1+p_2 > p_3$, $0 < p_1 < p_2 < p_3 < p_1+p_2$. Because of $p_3-p_2 > \hat{d}$ and $p_1+p_2-p_3 > \hat{d}$, $p_1 > 2\hat{d}$. Then $p_3 > p_1+2\hat{d} > 4\hat{d}=2\Psi_{s_3}$ which is still a contradiction. Hence $d_{opt}=\frac{1}{2}\Psi_{s_3}$.

When $\frac{\Psi_{s_4}}{8}=\min\left(\Psi_{s_1}, \frac{\Psi_{s_2}}{2}, \frac{\Psi_{s_3}}{4}, \frac{\Psi_{s_4}}{8}\right)$, there is $d_{opt}=\frac{1}{4}\Psi_{s_4}$, $0 < p_1 < p_2 < p_3 < p_4$. If $p_1+p_2+p_3 < p_4$, p_4 would become the ninth constellation point then $p_4 > 8\hat{d}=2\Psi_{s_4}$ which is a contradiction. If $p_1+p_2+p_3 > p_4$, there are two different cases as follows:

Case 1: $p_1+p_2 < p_3$. It could be derive that $0 < p_1 < p_2 < p_1+p_2 < p_3 < p_1+p_3 < p_2+p_3 < p_1+p_2+p_3$. According to the possible values of p_4, there are several different situations,

1) $p_2+p_3 < p_4 < p_1+p_2+p_3$. $p_1=p_1+p_2+p_3-(p_2+p_3) > 2\hat{d}$, we could derive $p_4 > p_1+6\hat{d} > 8\hat{d}=2\Psi_{s_4}$ which is a contradiction. Hence $d_{opt}=\frac{1}{4}\Psi_{s_4}$.

2) $p_1+p_3 < p_4 < p_2+p_3$. We can get $p_1+p_4 < p_1+p_2+p_3$. Then, $p_1+p_2+p_3-(p_1+p_2) > 6\hat{d}$, so $p_4 > p_3+2\hat{d} > 8\hat{d}=2\Psi_{s_4}$ which is a contradiction. Hence $d_{opt}=\frac{1}{4}\Psi_{s_4}$.

3) $p_3 < p_4 < p_1+p_3$. We can get $p_1+p_4, p_2+p_4 < p_1+p_2+p_3$. Then, $p_1+p_2+p_3-(p_1+p_2) > 7\hat{d}$, so $p_4 > p_3+\hat{d} > 8\hat{d}=2\Psi_{s_4}$ which is a contradiction. Hence $d_{opt}=\frac{1}{4}\Psi_{s_4}$.

Case 2: $p_3 < p_1+p_2$. It could be derived that $0 < p_1 < p_2 < p_3 < p_1+p_2 < p_1+p_3 < p_2+p_3 < p_1+p_2+p_3$. According to the possible values of p_4, there are also several different situations,

1) $p_2+p_3 < p_4 < p_1+p_2+p_3$. We can get $p_1+p_3-p_2 > 3\hat{d}$. Then $p_3 > p_2-p_1+3\hat{d} > 4\hat{d}$, so $p_4 > p_3+4\hat{d}=8\hat{d}$, which is a contradiction. Hence $d_{opt}=\frac{1}{4}\Psi_{s_4}$.

2) $p_1+p_3 < p_4 < p_2+p_3$. We can get $p_2+p_3-p_4 > \hat{d}$. Then $p_2 > p_4-p_3+\hat{d} > 4\hat{d}$, so $p_4 > p_2+4\hat{d}=8\hat{d}$ which is a contradiction. Hence $d_{opt}=\frac{1}{4}\Psi_{s_4}$.

3) $p_1+p_2 < p_4 < p_1+p_3$. We can get $p_1+p_3-p_4 > \hat{d}$ Then $p_1 > p_4-p_3+\hat{d} > 3\hat{d}$, $p_2 > p_1+\hat{d} > 4\hat{d}$, so $p_4 > p_1+p_2+\hat{d} > 3\hat{d}+4\hat{d}+\hat{d}=8\hat{d}$ which is a contradiction. Hence $d_{opt}=\frac{1}{4}\Psi_{s_4}$.

4) $p_3 < p_4 < p_1+p_2$. According to the values of p_2+p_3 and p_1+p_4, there are two different situations,

(a) $0 < p_1 < p_2 < p_3 < p_4 < p_1+p_2 < p_1+p_3 < p_2+p_3 < p_1+p_4 < p_1+p_2+p_3$. $(p_1+p_4)-p_4 > 4\hat{d}$, then $p_1 > 4\hat{d}$. $p_1+p_4-(p_1+p_3) > 2\hat{d}$, so $p_4 > p_3+2\hat{d} > p_1+2\hat{d}+2\hat{d} > 4\hat{d}+2\hat{d}+2\hat{d}=8\hat{d}$, which is a contradiction. Hence $d_{opt}=\frac{1}{4}\Psi_{s_4}$.

(b) $0 < p_1 < p_2 < p_3 < p_4 < p_1+p_2 < p_1+p_3 < p_1+p_4 < p_2+p_3 < p_1+p_2+p_3$. Unlike aforementioned cases, there is no contradiction could be derived in this scenario. Here we can get the entire order of constellation points, then the objective function in Eq. (8) could be rewritten as $\max_{\mathbf{p}} \min(p_1, p_2-p_1, p_3-p_2, p_4-p_3, p_1+p_2-p_4, p_2+p_3-p_1-p_4)$. Because of $p_1 > p_1+p_2-p_4$ and $p_2-p_1 > p_2+p_3-p_1-p_4$, the objective function is further simplified as $\max_{\mathbf{p}} \min(p_3-p_2, p_4-p_3, p_1+p_2-p_4, p_2+p_3-p_1-p_4)$. If $\min_{\mathbf{e}} d=p_3-p_2$, the same as proof of theorem 1, this linear programming problem can be written as

$$\begin{aligned} \text{LP2}: \quad & \max\ p_3-p_2 \\ & \text{s.t. } p_3-p_2 < p_4-p_3, \\ & \quad p_3-p_2 < p_1+p_2-p_4, \\ & \quad p_3-p_2 < p_2+p_3-p_1-p_4. \end{aligned} \tag{15}$$

It is easy to confirmed that the maximized d of this LP problem is obtained at the basic feasible solution $\mathbf{p} = [1, \frac{5}{3}, 2, \frac{7}{3}]^T p_1$. As well, if $\min_{\mathbf{e}} d = p_4 - p_3$ or $\min_{\mathbf{e}} d = p_1 + p_2 - p_4$ or $\min_{\mathbf{e}} d = p_2 + p_3 - p_1 - p_4$, we could also get the same results. Hence the optimal value of d is $d_{opt} = \frac{1}{3}p_1$. This question is further simplified as maximizing p_1 subject to $\psi_{d_1} + \frac{1}{2}p_1 = \Psi_{s_1}$, $\psi_{d_2} + \frac{5}{6}p_1 = \Psi_{s_2}$, $\psi_{d_3} + p_1 = \Psi_{s_3}$, $\psi_{d_4} + \frac{7}{6}p_1 = \Psi_{s_4}$ and $\psi_{d_1}, \psi_{d_2}, \psi_{d_3}, \psi_{d_4} \geqslant 0$. These constraints can be transferred to $0 < p_1 \leqslant \min\left(2\Psi_{s_1}, \frac{6}{5}\Psi_{s_2}, \Psi_{s_3}, \frac{6}{7}\Psi_{s_4}\right)$. Therefore, as we set $\mathbf{c} = \left[1, \frac{5}{3}, 2, \frac{7}{3}\right]^T$, when $\frac{\Psi_{s_i}}{c_i} = \min\left(\Psi_{s_1}, \frac{3}{5}\Psi_{s_2}, \frac{1}{2}\Psi_{s_3}, \frac{3}{7}\Psi_{s_4}\right)$, the optimal $\mathbf{p}^* = \mathbf{c} \cdot \frac{2\Psi_{s_i}}{c_i}$, $\boldsymbol{\psi}_{\boldsymbol{d}}^* = \boldsymbol{\Psi}_{\mathbf{s}} - \mathbf{c} \cdot \frac{\Psi_{s_i}}{c_i}$ and $d_{opt} = \frac{2}{3c_i}\Psi_{s_i}$. So the optimal $\mathbf{q}^* = \mathbf{c} \cdot \frac{2\Psi_{s_i}}{c_i h_i}$, $\boldsymbol{\phi}_{\boldsymbol{d}}^* = \boldsymbol{\Phi}_{\mathbf{s}} - \mathbf{c} \cdot \frac{\Psi_{s_i}}{c_i h_i}$.

As a result, the linear optimal signal structure in $N = 4$ when $\frac{\Psi_{s_4}}{8} = \min\left(\Psi_{s_1}, \frac{\Psi_{s_2}}{2}, \frac{\Psi_{s_3}}{4}, \frac{\Psi_{s_4}}{8}\right)$ is determined by the value of $\frac{1}{4}\Psi_{s_4}$ and $\frac{2}{3c_i}\Psi_{s_i}$.

If $\Psi_{s_4} \geqslant \frac{8}{3c_i}\Psi_{s_i}$, i.e., $\frac{1}{4}\Psi_{s_4} \geqslant \frac{2}{3c_i}\Psi_{s_i}$, the optimal constellation distances are equivalent. $\mathbf{p}^* = \mathbf{w} \cdot \frac{\Psi_{s_4}}{4}$, $\boldsymbol{\psi}_{\boldsymbol{d}}^* = \boldsymbol{\Psi}_{\mathbf{s}} - \mathbf{w} \cdot \frac{\Psi_{s_4}}{8}$, $\mathbf{w} = [1, 2, 4, 8]^T$, and $d_{opt} = \frac{\Psi_{s_4}}{4}$. So the optimal $\mathbf{q}^* = \mathbf{w} \cdot \frac{\Psi_{s_4}}{4h_i}$ and $\boldsymbol{\phi}_{\boldsymbol{d}}^* = \boldsymbol{\Phi}_{\mathbf{s}} - \mathbf{w} \cdot \frac{\Psi_{s_4}}{8h_i}$.

If $\Psi_{s_4} < \frac{8}{3c_i}\Psi_{s_i}$, i.e., $\frac{1}{4}\Psi_{s_4} < \frac{2}{3c_i}\Psi_{s_i}$, the optimal constellation distances are in-equivalent. $\mathbf{p}^* = \mathbf{c} \cdot \frac{2\Psi_{s_i}}{c_i}$, $\boldsymbol{\psi}_{\boldsymbol{d}}^* = \boldsymbol{\Psi}_{\mathbf{s}} - \mathbf{c} \cdot \frac{\Psi_{s_i}}{c_i}$, $\mathbf{c} = \left[1, \frac{5}{3}, 2, \frac{7}{3}\right]^T$, and $d_{opt} = \frac{2}{3c_i}\Psi_{s_i}$. So the optimal $\mathbf{q}^* = \mathbf{c} \cdot \frac{2\Psi_{s_i}}{c_i h_i}$, $\boldsymbol{\phi}_{\boldsymbol{d}}^* = \boldsymbol{\Phi}_{\mathbf{s}} - \mathbf{c} \cdot \frac{\Psi_{s_i}}{c_i h_i}$.

Considering above two cases, there are only one situation in Case 2 which dissatisfy our initial assumption. After summarizing all the conclusions, the linear optimal signal structure for $N = 4$ is written as Theorem 2.

The proof of Theorem 2 is completed. □

REFERENCES

[1] H. Elgala, R. Mesleh, and H. Haas, "Indoor optical wireless communication: Potential and state-of-the-art," *IEEE Commun. Mag.*, vol. 49, no. 9, pp. 56–62, Sep. 2011.

[2] L. Grobe *et al.*, "High-speed visible light communication systems," *IEEE Commun. Mag.*, vol. 51, no. 11, pp. 60–66, Dec. 2013.

[3] P. H. Pathak, X. Feng, P. Hu, and P. Mohapatra, "Visible light communication, networking, and sensing: A survey, potential and challenges," *IEEE Commun. Surveys Tuts.*, vol. 17, no. 4, pp. 2047–2077, 4th Quart., 2015.

[4] A. Zukauskas, M. S. Shur, and R. Gaska, *Introduction to Solid-State Lighting*. New York, NY, USA: Wiley, 2002.

[5] T. Komine and M. Nakagawa, "Fundamental analysis for visible-light communication system using LED lights," *IEEE Trans. Consum. Electron.*, vol. 50, no. 1, pp. 100–107, Feb. 2004.

[6] Z. Wang, C. Yu, W.-D. Zhong, J. Chen, and W. Chen, "Performance of a novel LED lamp arrangement to reduce SNR fluctuation for multi-user visible light communication systems," *Opt. Express*, vol. 20, no. 4, pp. 4564–4573, Feb. 2012.

[7] D.-F. Zhang, Y.-J. Zhu, J.-K. Zhang, and Y.-Y. Zhang, "Constellation collaborated OFDM for visible light communication systems," *IEEE Commun. Lett.*, vol. 18, no. 6, pp. 1067–1070, Jun. 2014.

[8] Y. J. Zhu, W. Y. Wang, and G. Xin, "Faster-than-Nyquist signal design for multiuser multicell indoor visible light communications," *IEEE Photon. J.*, vol. 8, no. 1, pp. 1–12, Feb. 2016.

[9] Z.-G. Sun, H.-Y. Yu, Y.-J. Zhu, and Z.-J. Tian, "An addition-decomposable relaying protocol and signal design for optical wireless communications," *IEEE Trans. Veh. Technol.*, vol. 67, no. 7, pp. 5980–5993, Jul. 2018.

[10] D. Karunatilaka, F. Zafar, V. Kalavally, and R. Parthiban, "LED based indoor visible light communications: State of the art," *IEEE Commun. Surveys Tuts.*, vol. 17, no. 3, pp. 1649–1678, 3rd Quart., 2015.

[11] Y.-J. Zhu, W.-F. Liang, J.-K. Zhang, and Y.-Y. Zhang, "Space-collaborative constellation designs for MIMO indoor visible light communications," *IEEE Photon. Technol. Lett.*, vol. 27, no. 15, pp. 1667–1670, Aug. 1, 2015.

[12] Y.-Y. Zhang, H.-Y. Yu, J.-K. Zhang, Y.-J. Zhu, J.-L. Wang, and T. Wang, "Space codes for MIMO optical wireless communications: Error performance criterion and code construction," *IEEE Trans. Wireless Commun.*, vol. 16, no. 5, pp. 3072–3085, May 2017.

[13] Y.-Y. Zhang, H.-Y. Yu, J.-K. Zhang, Y. J. Zhu, J. L. Wang, and X. S. Ji, "On the optimality of spatial repetition coding for MIMO optical wireless communications," *IEEE Commun. Lett.*, vol. 20, no. 5, pp. 846–849, May 2016.

[14] R. Wang *et al.*, "Linear transceiver designs for MIMO indoor visible light communications under lighting constraints," *IEEE Trans. Commun.*, vol. 65, no. 6, pp. 2494–2508, Jun. 2017.

[15] C. Gong, S. Li, Q. Gao, and Z. Xu, "Power and rate optimization for visible light communication system with lighting constraints," *IEEE Trans. Signal Process.*, vol. 63, no. 16, pp. 4245–4256, Aug. 2015.

[16] T. Xiao, C. Gong, Q. Gao, and Z. Xu, "Channel characterization for multi-color VLC for feedback and beamforming design," in *Proc. IEEE ICC Workshop Opt. Wireless Commun.*, May 2018, pp. 1–6.

[17] K.-H. Park, Y.-C. Ko, and M.-S. Alouini, "On the power and offset allocation for rate adaptation of spatial multiplexing in optical wireless MIMO channels," *IEEE Trans. Commun.*, vol. 61, no. 4, pp. 1535–1543, Apr. 2013.

[18] R. Jiang, Z. Wang, Q. Wang, and L. Dai, "Multi-user sum-rate optimization for visible light communications with lighting constraints," *J. Lightw. Technol.*, vol. 34, no. 16, pp. 3943–3952, Aug. 15, 2016.

[19] J. Dong, Y. Zhang, and Y. Zhu, "Convex relaxation for illumination control of multi-color multiple-input-multiple-output visible light communications with linear minimum mean square error detection," *Appl. Opt.*, vol. 56, no. 23, pp. 6587–6595, Aug. 2017.

[20] Y. Y. Zhang, H.-Y. Yu, and J.-K. Zhang, "Block precoding for peak-limited MISO broadcast VLC: Constellation-optimal structure and addition-unique designs," *IEEE J. Sel. Areas Commun.*, vol. 36, no. 1, pp. 78–90, Jan. 2017.

[21] R. D. Roberts, S. Rajagopal, and S.-K. Lim, "IEEE 802.15.7 physical layer summary," in *Proc. GLOBECOM Workshops*, Dec. 2011, pp. 772–776.

[22] R. Singh, T. O'Farrell, and J. P. R. David, "Performance evaluation of IEEE 802.15.7 CSK physical layer," in *Proc. GLOBECOM Workshops*, Dec. 2013, pp. 1064–1069.

[23] E. Monteiro and S. Hranilovic, "Design and implementation of color-shift keying for visible light communications," *J. Lightw. Technol.*, vol. 32, no. 10, pp. 2053–2060, Mar. 15, 2014.

[24] R. Singh, T. O'Farrell, and J. P. R. David, "Analysis of forward error correction schemes for colour shift keying modulation," in *Proc. IEEE Int. Symp. Pers., Indoor, Mobile Radio Commun.*, Aug./Sep. 2015, pp. 575–579.

[25] R. Singh, T. O'Farrell, and J. P. R. David, "An enhanced color shift keying modulation scheme for high-speed wireless visible light communications," *J. Lightw. Technol.*, vol. 32, no. 14, pp. 2582–2592, Jul. 15, 2014.

[26] X. Liang, M. Yuan, J. Wang, Z. Ding, M. Jiang, and C. Zhao, "Constellation design enhancement for color-shift keying modulation of quadrichromatic LEDs in visible light communications," *J. Lightw. Technol.*, vol. 35, no. 17, pp. 3650–3663, Sep. 1, 2017.

[27] J.-M. Dong, Y.-J. Zhu, Y.-Y. Zhang, and Z.-G. Sun, "Illumination-adapted transceiver design for quadrichromatic light-emitting diode based visible light communication," *IEEE Photon. J.*, vol. 10, no. 3, Jun. 2018, Art. no. 7904010.

[28] J.-M. Dong, Y.-J. Zhu, and Z.-G. Sun, "Adaptive multi-color shift keying constellation design for visible light communications considering lighting requirement," *Opt. Commun.*, vol. 430, no. 3, pp. 293–298, Jan. 2018.

[29] K.-I. Ahn and J. K. Kwon, "Color intensity modulation for multicolored visible light communications," *IEEE Photon. Technol. Lett.*, vol. 24, no. 24, pp. 2254–2257, Dec. 15, 2012.

[30] T. Smith and J. Guild, "The C.I.E. colorimetric standards and their use," *Trans. Opt. Soc.*, vol. 33, no. 3, p. 73, Jan. 2002.

[31] D. H. Krantz, "Color measurement and color theory: II. Opponent-colors theory," *J. Math. Psychol.*, vol. 12, no. 3, pp. 304–327, Aug. 1975.

[32] G. Wyszecki and W. S. Stiles, *Color Science: Concepts and Methods, Quantitative Data and Formulae*, 2nd ed. New York, NY, USA: Wiley, 1982.
[33] *ANSI NEMA ANSLG C78.377-2008: Specications for the Chromaticity of Solid State Lighting Products*, ANSI, Washington, DC, USA, 2008.
[34] A. Chaaban, Z. Rezki, and M.-S. Alouini, "Fundamental limits of parallel optical wireless channels: Capacity results and outage formulation," *IEEE Trans. Commun.*, vol. 65, no. 1, pp. 296–311, Jan. 2007.
[35] L. Zeng *et al.*, "High data rate multiple input multiple output (MIMO) optical wireless communications using white LED lighting," *IEEE J. Sel. Areas Commun.*, vol. 27, no. 9, pp. 1654–1662, Dec. 2009.
[36] T. Fath and H. Haas, "Performance comparison of MIMO techniques for optical wireless communications in indoor environments," *IEEE Trans. Commun.*, vol. 61, no. 2, pp. 733–742, Feb. 2013.
[37] S. Sayegh, "A condition for optimality of two-dimensional signal constellations," *IEEE Trans. Commun.*, vol. COMM-33, no. 11, pp. 1220–1222, Nov. 1985.
[38] H. Flanders and J. J. Price, *Calculus With Analytic Geometry*. New York, NY, USA: Academic, 1978.
[39] B. M. Alzalg, "Stochastic second-order cone programming: Applications models," *Appl. Math. Modell.*, vol. 36, no. 10, pp. 5122–5134, Oct. 2012.
[40] M. Grant, S. Boyd, and Y. Ye, "CVX: MATLAB software for disciplined convex programming," Jun. 2015. [Online]. Available: http://cvxr.com/cvx/
[41] Y. Ye, *Interior Point Algorithms: Theory and Analysis*. Hoboken, NJ, USA: Wiley, 1997.
[42] *ANSI NEMA ANSLG C78.376-2001: Specications for the Chromaticity of Fluorescent Lamps*, ANSI, Washington, DC, USA, 2001.
[43] W.-Y. Wang and Y.-J. Zhu, "A multi-LED collaborated signal design for MISO VLC systems based on amplitude-phase superposition," *IEEE Photon. J.*, vol. 8, no. 5, Sep. 2017, Art. no. 7804309.
[44] D. Bertsimas and J. Tsitsiklis, *Introduction to Linear Optimization*. Belmont, MA, USA: Athena Scientific, 1997.

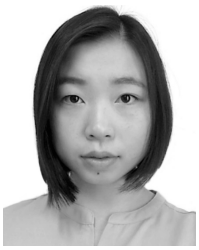

YE XIAO received the B.S. degree from the National Digital Switching System Engineering and Technological Research Center, Zhengzhou, Henan, China, in 2016, where she is currently pursuing the M.S. degree. Her main research interests are in the areas of wireless communication theory, visible light communications, and signal processing.

YI-JUN ZHU (M'14) received the B.Eng., M.Sc., and Ph.D. degrees from the National Digital Switching System Engineering and Technological Research Center (NDSC), Zhengzhou, Henan, China, in 1999, 2002, and 2010, respectively. In 2011, he visited the Department of Electrical and Computer Engineering, McMaster University. He is currently with NDSC. His main research interests are in the areas of wireless communication theory, visible light communications, and signal processing.

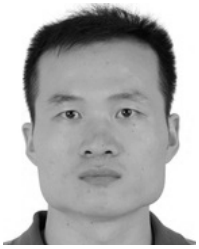

YAN-YU ZHANG received the B.S. degree in communication engineering, the M.S. degree in communication and information system, and the Ph.D. degree in information and communication engineering from the National Digital Switching System Engineering and Technological Research Center (NDSC), Zhengzhou, China, in 2009, 2012, and 2016, respectively. He is currently a Lecturer with NDSC. His research interests lie in the finitealphabet signal processing for radio frequencys or optical wireless communications with current focus on the fundamental structure establishment and energy-efficient designs for multiuser finite-alphabet signals.

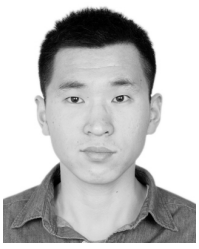

ZHENG-GUO SUN received the B.Eng. and M.Sc. degrees from the National Digital Switching System Engineering and Technological Research Center, Zhengzhou, Henan, China, in 2012 and 2015, respectively, where he is currently pursuing the Ph.D. degree. His main research interests include wireless communication theory, visible light communications, and signal processing.